Research in Astronomy and Astrophysics, 22:015013 (11pp), 2022 January https://doi.org/10.1088/1674-4527/ac37b4

Analysis of TESS Field Eclipsing Binary Star V948 Her: A Pulsating or Non-pulsating Star?

F Kahraman Aliçavuş[1,2] and Ö Ekinci[2,3]
[1] Çanakkale Onsekiz Mart University, Faculty of Sciences and Arts, Physics Department, 17100, Çanakkale, Turkey; filizkahraman01@gmail.com
[2] Çanakkale Onsekiz Mart University, Astrophysics Research Center and Ulupınar Observatory, TR-17100, Çanakkale, Turkey
[3] Çanakkale Onsekiz Mart University, School of Graduate Studies, Department of Space Sciences and Technologies, TR-17100, Çanakkale, Turkey
Received 2021 August 16; revised 2021 October 21; accepted 2021 November 8; published 2022 January 21

Abstract

Pulsating stars occupy a significant place in the H-R diagram and it was thought that all stars inside the classical instability strip should pulsate. However, recent studies showed that there are many non-pulsating stars located inside the classical instability strip. The existence of these non-pulsating stars is still a mystery. To deeply understand the properties of these non-pulsating and pulsating stars, one needs precise fundamental stellar parameters (e.g. mass). For this purpose, the eclipsing binaries are unique systems. Hence, in this study, we present the TESS data analysis of one candidate pulsating eclipsing binary system, V948 Her. TESS data were used for the binary modeling with the literature radial velocity measurements, and the precise fundamental parameters of the system were obtained. The system's age was derived as 1 ± 0.24 Gyr. The positions of the binary components in the H-R diagram were examined and the primary component was found inside the δ Scuti instability strip. However, in the frequency analysis of TESS data, we found no significant pulsation frequencies. Only the harmonics of the orbital periods were obtained in the analysis. Therefore, the system was classified as a non-pulsator. V948 Her is an important object to understand the nature of non-pulsating stars inside the δ Scuti instability strip.

Key words: (stars:) binaries: eclipsing – stars: fundamental parameters – techniques: photometric

1. Introduction

Space-based observations have significantly contributed to astrophysical investigations. In particular, recent space missions such as CoRoT (Baglin et al. 2006), Kepler (Borucki et al. 2010) and Transiting Exoplanet Survey Satellite (TESS, Ricker et al. 2014) have provided high-quality photometric data of many stellar objects. Thanks to these data, the characteristics of many stellar systems have been revealed, while some new mysteries about them have come along.

High-quality space data have created a revolution in the studies of pulsating and binary stars. Binary systems, particularly eclipsing binary stars, are unique systems to directly and sensitively derive the fundamental stellar parameters of mass (M) and radius (R). These fundamental stellar parameters could be obtained with an accuracy of $\sim$1% with the simultaneous analysis of light and radial velocity (v_r) curves (Torres et al. 2010). Spaced-based photometric observations have increased the sensitivity of these parameters with their high-precision data (Maxted et al. 2020). Precise fundamental stellar parameters are substantial for an extensive examination and understanding of the stellar evolution and calibrating the theoretical models (Tkachenko et al. 2020). In eclipsing binary systems, these space-based data have also disclosed some out-of-eclipse variations which could not be detected from ground-based studies. Those variations could be the results of stellar spots and/or pulsations in the binary component(s) (Pan et al. 2020; Maxted et al. 2020). Additionally, it was also reported that these out-of-eclipse variations could be the effect of Doppler-beaming caused by the orbital motion of the binary components (Herrero et al. 2014; Eigmüller et al. 2018). A comprehensive investigation of these out-of-eclipse variations could give us more information about the stellar systems such as about their interior structure with the help of pulsation modes.

Pulsating binary systems have been known for decades. These systems occupy a notable place in astrophysical investigations because of their pulsation and eclipsing characteristics. The research on pulsations provides us information about the interior structure of stars, while studies of eclipsing binaries help us to determine the precise fundamental parameters. Therefore, the combination of these two properties creates a particular tool in investigating stellar structure and evolution. Examinations of high-quality space-based data have shown us that the pulsation characteristics of some oscillating stars could not have been fully discerned yet (Antoci et al. 2014; Bowman & Kurtz 2018). There are some open questions, especially about the A-F type δ Scuti and γ Doradus pulsators. In the study of Uytterhoeven et al. (2011), about 750 Kepler field δ Scuti, γ Doradus stars and their hybrids were examined and it turned out that there are some pulsating stars

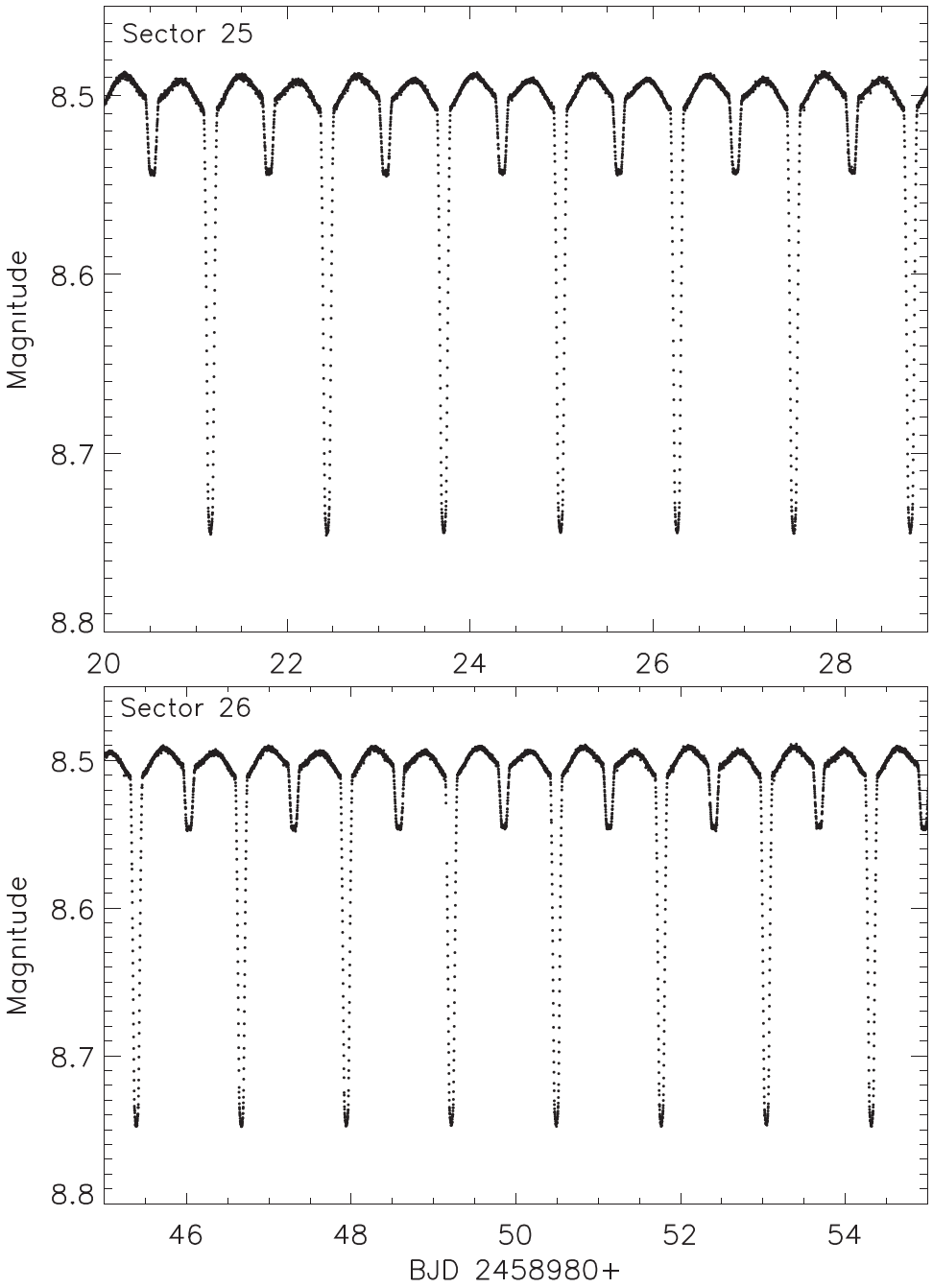

Figure 1. Light curve of ∼10-days from sector 25 and 26 observations.

located beyond their own instability strips. This result conflicts with the theoretical studies because theoretically, these pulsating stars should not exhibit their kind of oscillations out of their own domain. The other interesting thing is that some non-pulsators were found inside the instability strip of these oscillating stars (Uytterhoeven et al. 2011). Breger suggested that probably all stars inside the classical instability strip manifest oscillations but some of them have a very low amplitude which could not be detected from ground-based observations because of the accuracy of the observations (Breger 1969). However, recent studies with space-based photometric data indicated that there are non-pulsators inside the instability strips of these variables (Guzik et al. 2013;

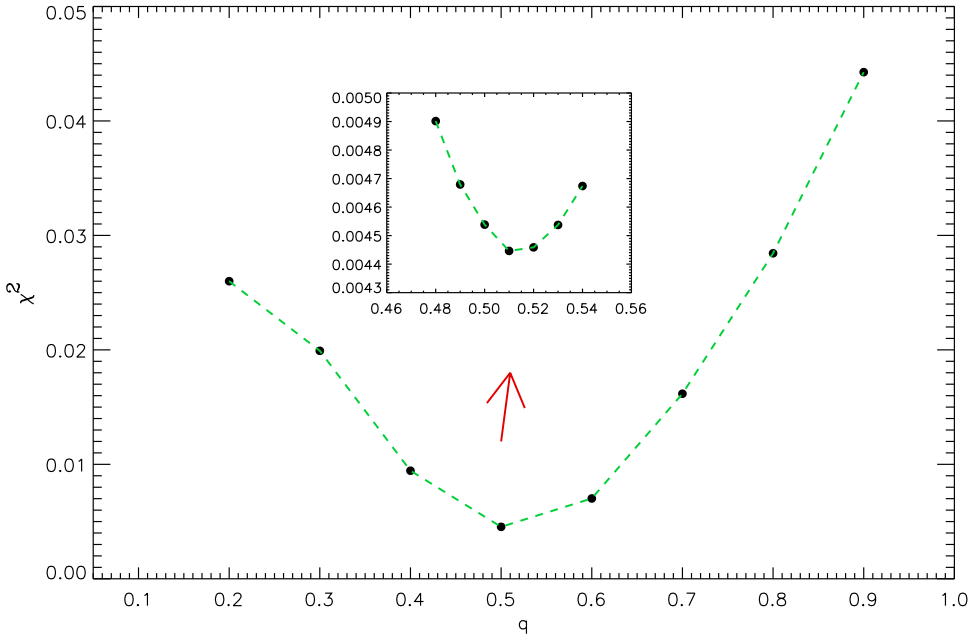

Figure 2. Results for the q search.

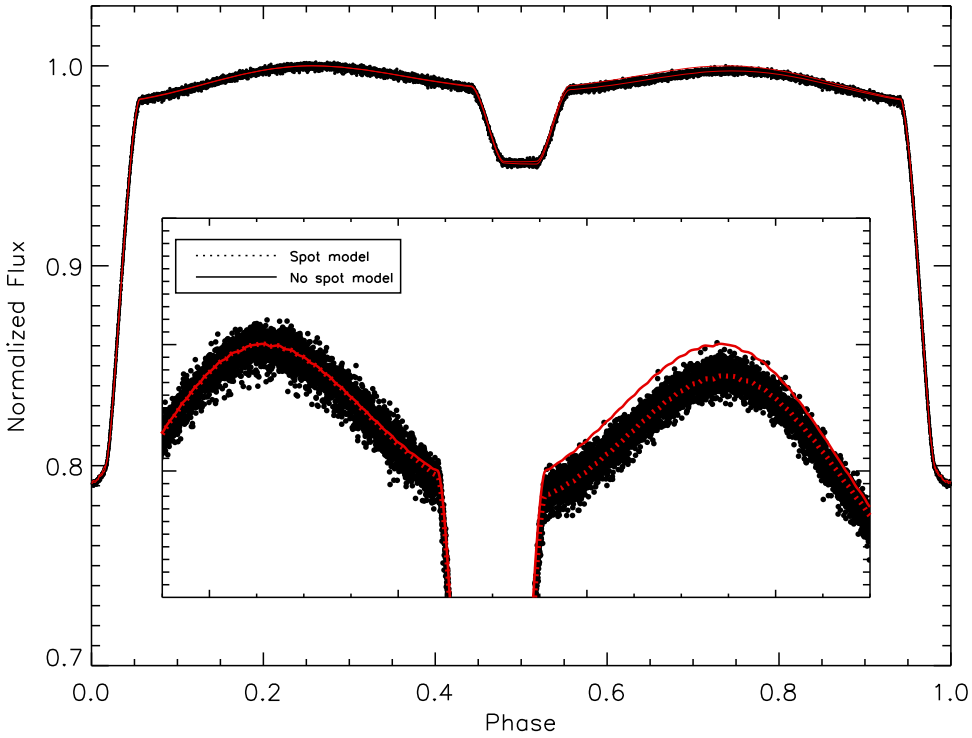

Figure 3. Theoretical fits (red lines) to the TESS phased data and the consistency of the spotted model (dotted line).

Murphy et al. 2015; Narloch et al. 2019). In a recent study, Murphy et al. (2019) examined the fraction of pulsators inside the δ Scuti instability strip. This fraction was found to be decreasing through the red and blue edges, while it reached 70% in the middle of the δ Scuti instability strip. It was clearly shown that there are some stars in the δ Scuti instability strip and they exhibit no oscillations at the micromagnitude sensitivity level of TESS data. The secret of these non-pulsators still remains, although studies

were carried out about these systems (Balona & Dziembowski 2011; Guzik et al. 2013; Murphy et al. 2015; Narloch et al. 2019). To understand the mysteries of these non-pulsators, the eclipsing binary systems with non-pulsating or pulsating component(s) inside the δ Scuti instability strip could be useful. Therefore, in this study, we focused on the analysis of an eclipsing binary system, V948 Her, which is believed to have a candidate δ Scuti binary component.

The eclipsing variability of V948 Her was found by Hipparcos (ESA 1997). The primary component of the system was listed as a candidate pulsator by Soydugan et al. (2006). Liakos & Niarchos (2012) classified the system as a detached eclipsing binary and searched for possible pulsations by using ground-based observations. However, they found no convincing result. A comprehensive study of V948 Her was given by Kahraman Aliçavus (2018). In this work, the ELODIE spectra and the Super Wide Angle Search for Planets (SuperWASP) photometric data were used. The system was found to be a single-lined binary and the atmospheric parameters, projected rotational velocity ($v \sin i$) and metallicity (Fe/H) of the primary component were obtained by utilizing the available spectra. Simultaneous analysis of v_r and the associated light curve was presented. The author also pointed out that some oscillation-like behaviors in the SuperWASP data are available and more observations are needed to confirm this variability. To reveal and understand the out-of-eclipse variations in this system, high-precision photometric data are needed. Thanks to the TESS mission, now the system has high-quality photometric data and this allows us to probe the out-of-eclipse variations in this system, obtain precise fundamental stellar parameters and examine the evolution of the system. Therefore, a revised analysis of V948 Her is presented in this study. The paper is organized as follows. The information about the photometric data and new ephemeris calculation are given in Section 2. The binary modeling and time-series analysis are presented in the Section 3. The discussions and conclusion are provided in Section 4.

Table 1
Results of the Light Curve Analysis and the Fundamental Stellar Parameters

Parameter	Value (This Study)	Value (Kahraman Aliçavus 2018)
i (°)	85.518 ± 0.031	86.86 ± 0.044
T_1^a (K)	7100 ± 200	7100 ± 200
T_2 (K)	4280 ± 230	4430 ± 250
Ω_1	4.516 ± 0.004	4.521 ± 0.005
Ω_2	5.942 ± 0.006	5.584 ± 0.010
Phase shift	−0.0011 ± 0.0001	0.000 40 ± 0.00004
q	0.504 ± 0.001	0.443 ± 0.001
r_1[a] (mean)	0.2512 ± 0.0036	···
r_2[a] (mean)	0.1075 ± 0.0026	···
$l_1/(l_1+l_2)$	0.970 ± 0.013	0.981 ± 0.004
$l_2/(l_1+l_2)$	0.030 ± 0.016	0.019 ± 0.005
l_3	0.00	0.00
Spot Parameters		
Co-Latitude (deg)	90[a]	···
Longitude (deg)	114.340 ± 0.112	···
Radius (deg)	25.720 ± 0.038	···
Temperature Factor[b]	0.995 ± 0.003	···
Derived Quantities		
M_1 ($M_\odot$)	1.274 ± 0.012	1.722 ± 0.123
M_2 ($M_\odot$)	0.642 ± 0.014	0.762 ± 0.020
R_1 ($R_\odot$)	1.543 ± 0.022	1.655 ± 0.034
R_2 ($R_\odot$)	0.661 ± 0.016	0.689 ± 0.016
log ($L_1/L_\odot$)	0.737 ± 0.028	0.797 ± 0.034
log ($L_2/L_\odot$)	−0.880 ± 0.034	−0.783 ± 0.016
log g_1 (cgs)	4.16 ± 0.02	4.23 ± 0.10
log g_2 (cgs)	4.60 ± 0.03	4.63 ± 0.10
$M_{bol\ 1}$ (mag)	2.898 ± 0.082	2.763 ± 0.691
$M_{bol\ 2}$ (mag)	6.939 ± 0.104	6.715 ± 1.327
$M_{V\ 1}$ (mag)	2.820 ± 0.086	···
$M_{V\ 2}$ (mag)	7.534 ± 0.113	···

Notes.
[a] Fractional radii,
[b] $T_{eff,spot}/T_{eff,star}$.

2. Photometric Data and New Ephemeris Calculation

V948 Her was observed with TESS. TESS was originally designed for discovering new exoplanets orbiting around bright stars ($4 < I_c < 13$) in the sky. TESS has carried out its missions by dividing the sky into 26 partly overlapping sectors. Each of these sectors was observed around 27 days with 2 minute short cadence (SC) and 30 minute long cadence (LC) observation modes in a wide bandpass ranging from 600 to 10 000 nm (Ricker et al. 2014). The mission completed its 2 yr primary missions and continues an extended mission now.

During the first two years, TESS monitored V948 Her in two continuous sectors, 25 and 26, in 2 minute SC mode. In the study, we search for possible δ Scuti type pulsations in the system, therefore all SC data were taken into account. The SC data are more suitable for the asteroseismology of δ Scuti stars because its Nyquist frequency reaches around 340 d^{-1}. The SC data of V948 Her were taken from the Mikulski Archive for Space Telescopes (MAST) archive.[4] The PDC_SAP fluxes were converted into magnitudes and points scattered over 2σ were cleaned from the data. The PDC_SAP data of sectors 25 and 26 for around 10 continuous days are displayed in Figure 1. As clearly seen from the figure, there are asymmetries on the out-of-eclipse light curve and these could be the effect of a spot(s) located on the binary component(s).

The system was also observed at the Çanakkale Onsekiz Mart University Observatory with the Apogee ALTA U47 CCD

[4] https://mast.stsci.edu/

camera placed on the 30 cm telescope to obtain a new minimum time. We observed the primary minimum on 2021 July 9 with *V*-band. The photometric data were reduced by following the classical reduction steps (bias, dark subtraction and flat correction) with the C-Munipack[5] software. The new HJD minimum time was calculated to be 2 459 405.406 76 ± 0.0002 using the method of Kwee & van Woerden (1956). Additionally, we calculated the minima times from TESS and also available SuperWASP data of the system to examine its period variations. The primary and secondary minima times were derived from the first, middile and last parts of each TESS sector. In total, twelve TESS minima times were obtained. We also gathered three primary minima times from the SuperWASP data. The literature minima times of V948 Her were also collected from the O-C Gateway.[6] In total, we used 26 minima times and investigated the period changes of the system. All considered minima times are listed in Table A1. Those minima times were first investigated with the method of Zasche et al. (2009). According to our initial examination, we found that the system shows a 1.13 s period decrease in one hundred years. However, because of the fewer minima times, this result was not reliable and the system needs more minima times to obtain more decent results. For this reason, in this study, we only determined new light elements of V948 Her by finding a linear fit to all minima times. The new light elements are given in the following equation:

$$\mathrm{HJD(MIN}I) = 2459405.4012(7) + 1.275\,204\,9E(3) \quad (1)$$

3. Binary Modeling and Frequency Analysis

In the binary modeling of V948 Her, we controlled the level of maximum points in all available TESS SC data to check whether they show differences from one sector to the other. No significant variation was found. Therefore, we used only the data of sector 25 in the binary modeling. These data were binned to 4000 points. The Wilson-Devinney code (Wilson & Devinney 1971) with the Monte-Carlo simulation (Zola et al. 2004; Zola et al. 2010) was utilized in the study to derive reliable uncertainties in the searched parameters.

In the binary modeling, the effective temperature ($T_{\rm eff}$) of the primary (hot) binary component was taken to be 7100 ± 200 K from the results of the literature spectral analysis (Kahraman Aliçavus 2018) and this value was fixed during the analysis. The other fixed parameters are the bolometric albedos, bolometric gravity-darkening coefficient and the logarithmic limb darkening coefficient and they were taken the same as given in the study of Kahraman Aliçavus (2018). The previous binary modeling of the system was done with the SuperWASP data. As the TESS data are quite sensitive compared to SuperWASP, the binary parameters could be derived more accurately. Therefore, in the binary modeling, we searched for important binary parameters such as orbital inclination (i), mass ratio (q), surface potential (Ω) of the binary component and $T_{\rm eff}$ of the cool secondary component. As V948 Her is defined as a detached binary system (Liakos & Niarchos 2012; Kahraman Aliçavus 2018), a detached binary configuration was applied in the modeling.

Table 2
The Resulting Frequencies, Amplitudes and Phases for the Significant Frequencies

	Frequency (d^{-1})	Amplitude (mmag)	Phase (rad)	S/N
$46\nu_{\rm orb}$	36.0728(2)	0.358	0.573(2)	51.9
$44\nu_{\rm orb}$	34.5040(2)	0.331	0.222(3)	51.0
$48\nu_{\rm orb}$	37.6416(2)	0.308	0.924(3)	43.1
$47\nu_{\rm orb}$	36.8572(3)	0.233	0.253(4)	34.4
$45\nu_{\rm orb}$	35.2884(3)	0.232	0.908(4)	33.1
$42\nu_{\rm orb}$	32.9362(3)	0.215	0.849(4)	31.9
$36\nu_{\rm orb}$	28.2297(3)	0.197	0.313(4)	30.5
$50\nu_{\rm orb}$	39.2094(3)	0.196	0.299(4)	28.2
$49\nu_{\rm orb}$	38.4250(3)	0.188	0.630(5)	28.6
$43\nu_{\rm orb}$	33.7206(3)	0.187	0.528(5)	28.1
$35\nu_{\rm orb}$	27.4463(3)	0.186	0.601(5)	33.2
$33\nu_{\rm orb}$	25.8785(3)	0.185	0.207(5)	32.5
$34\nu_{\rm orb}$	26.6619(3)	0.184	0.941(5)	32.0
$37\nu_{\rm orb}$	29.0151(4)	0.136	0.940(6)	20.1
$51\nu_{\rm orb}$	39.9938(5)	0.121	0.969(7)	17.5
$38\nu_{\rm orb}$	29.7985(5)	0.116	0.582(7)	17.4
$72\nu_{\rm orb}$	56.4614(6)	0.109	0.794(8)	15.9
$74\nu_{\rm orb}$	58.0292(6)	0.103	0.188(8)	15.5
$52\nu_{\rm orb}$	40.7783(6)	0.100	0.642(9)	14.2
$70\nu_{\rm orb}$	54.8916(6)	0.100	0.472(9)	14.0
$41\nu_{\rm orb}$	32.1528(7)	0.090	0.145(10)	12.4
$73\nu_{\rm orb}$	57.2469(8)	0.074	0.411(11)	11.2
$76\nu_{\rm orb}$	59.5981(8)	0.072	0.528(12)	12.3
$75\nu_{\rm orb}$	58.8147(9)	0.071	0.809(12)	10.9
$53\nu_{\rm orb}$	41.5606(10)	0.064	0.420(13)	9.3
$71\nu_{\rm orb}$	55.6770(10)	0.060	0.086(14)	8.6
$68\nu_{\rm orb}$	53.3258(10)	0.059	0.020(15)	8.5
$40\nu_{\rm orb}$	31.3673(11)	0.053	0.487(16)	7.5
$69\nu_{\rm orb}$	54.1113(12)	0.051	0.672(17)	7.4
$60\nu_{\rm orb}$	47.0556(13)	0.047	0.975(18)	7.1
$98\nu_{\rm orb}$	76.8521(13)	0.046	0.926(19)	7.7
$77\nu_{\rm orb}$	60.3804(13)	0.045	0.256(19)	7.5
$62\nu_{\rm orb}$	48.6183(14)	0.045	0.509(19)	7.2
$59\nu_{\rm orb}$	46.2651(14)	0.043	0.454(20)	5.9
$96\nu_{\rm orb}$	75.2812(14)	0.037	0.633(20)	5.5
$61\nu_{\rm orb}$	47.8359(15)	0.042	0.791(21)	6.3
$99\nu_{\rm orb}$	77.6375(15)	0.041	0.596(21)	6.4
$78\nu_{\rm orb}$	61.1669(16)	0.039	0.874(22)	6.0
$39\nu_{\rm orb}$	30.5840(23)	0.032	0.346(33)	5.0
$64\nu_{\rm orb}$	50.1902(16)	0.037	0.760(23)	5.1
$97\nu_{\rm orb}$	76.0708(18)	0.034	0.169(26)	5.6
$100\nu_{\rm orb}$	78.4187(18)	0.034	0.276(25)	5.4
$55\nu_{\rm orb}$	43.1295(18)	0.034	0.742(25)	5.1
$102\nu_{\rm orb}$	79.9857(19)	0.032	0.754(27)	4.6
$54\nu_{\rm orb}$	42.3471(20)	0.031	0.061(28)	4.8
$101\nu_{\rm orb}$	79.2023(20)	0.030	0.057(28)	4.8
$63\nu_{\rm orb}$	49.4048(21)	0.029	0.101(30)	4.5

[5] http://c-munipack.sourceforge.net/
[6] http://var2.astro.cz/ocgate/

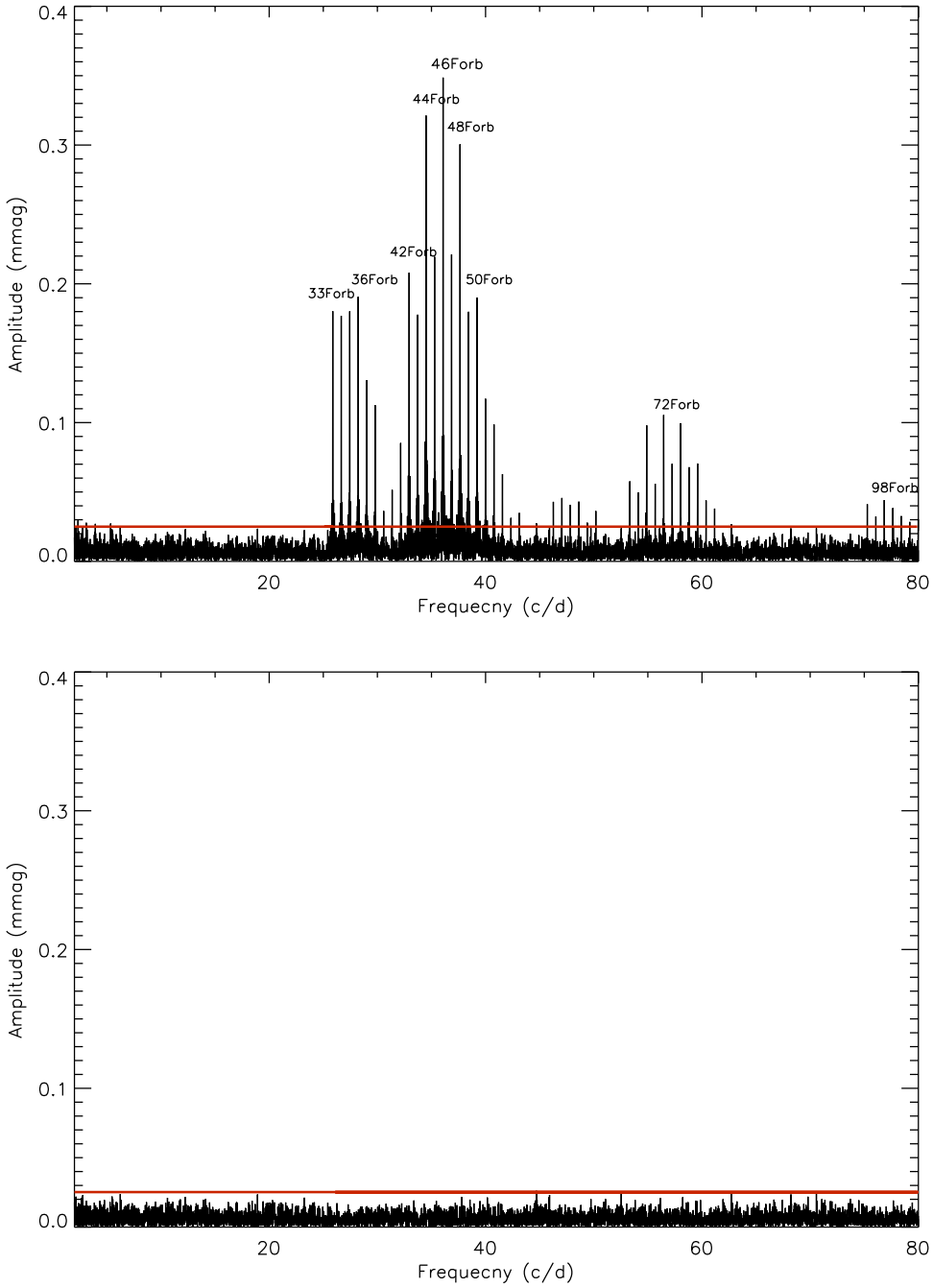

Figure 4. The Fourier spectrum of V948 Her (top panel). The horizontal red line represents the 4σ level. The bottom panel signifies the Fourier spectrum after prewhitening all significant harmonic frequencies of the orbital period.

We first carried out a model without assuming a spot on the system. However, the theoretical models without a spot did not represent the binary variation. Therefore, a spot was included in the binary modeling. First, a cool spot was assumed on the surface of the secondary cool star, however no significant results were obtained. Hence, new binary modeling was carried out by assuming a cool spot on the primary component. We obtained a better χ^2 value for the modeling with a cool spot on the surface of the primary component. As the system is a single-lined binary, we do not have precise information about the q value. Therefore, we carried out a q search to find the q value corresponding to

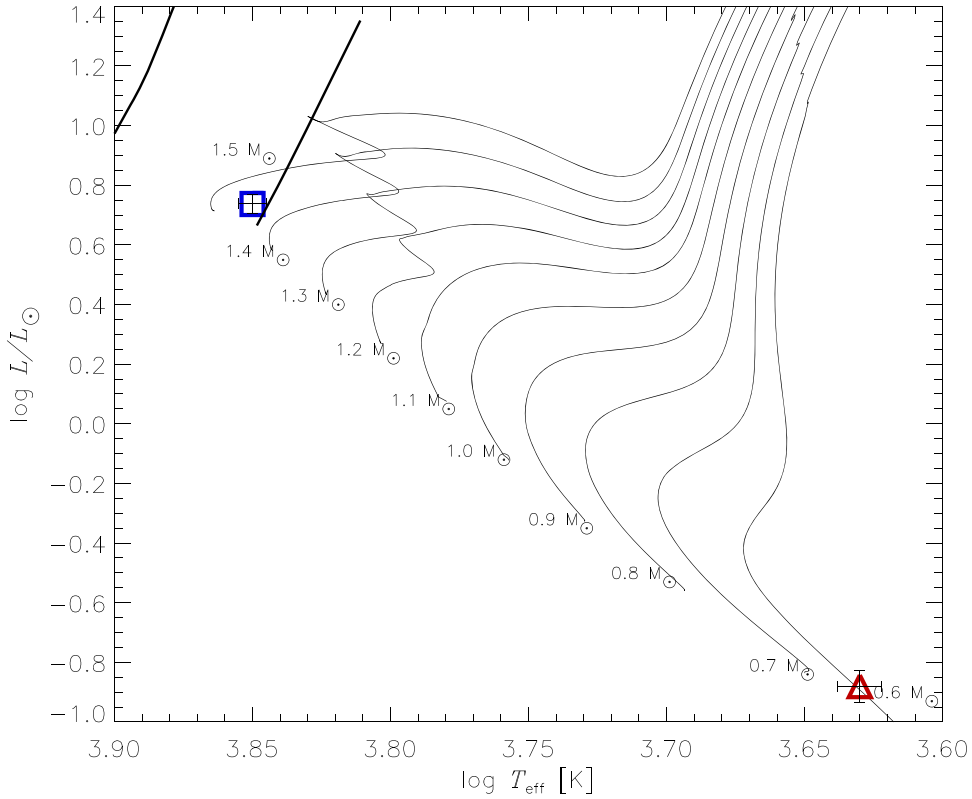

Figure 5. Position of the primary (square) and secondary (triangle) components of V948 Her in the H-R diagram and the δ Scuti instability strip (solid lines in the top-left) (Dupret et al. 2005).

the minimum χ^2. The result of this search is plotted in Figure 2. We obtained the minimum χ^2 for 0.51. Taking this q value as input, binary modeling was performed again and the results of this modeling are given in Table 1. The theoretical binary models with and without the spot are illustrated in Figure 3.

The updated binary modeling of V948 Her shows differences from the literature binary modeling (Kahraman Aliçavus 2018). The results of the previous binary modeling are also given in Table 1 for a comaprison. In particular, the Ω, q and fractional radius (r) differ significantly. These affect the resulting fundamental parameters. The discrepancy in the results of this and the previous binary modeling is expected because of the quality of data used in the analyses. That is why no spot was found in the previous binary modelings.

The fundamental stellar parameters M, R, luminosity (L), surface gravity ($\log g$) and bolometric ($M_{\rm bol}$) and absolute magnitudes (M_V) were calculated considering the mass function found in the radial velocity analysis (Kahraman Aliçavus 2018) and the binarity parameters obtained in this study. The resulting fundamental stellar parameters are given in Table 1. When the fundamental parameters are compared with the previously given ones in the literature (see Table 1), one could see that there are significant differences in those parameters and that would change the evolutionary scenario of the system and its position in the Hertzsprung–Russell (H-R) diagram.

The primary component of V948 Her was classified as a candidate δ Scuti star (Soydugan et al. 2006). In the study of Liakos & Niarchos (2012), no convincing frequency with a signal-to-noise ratio (S/N) larger than 4 was found. However, in the study of Kahraman Aliçavus (2018), the star is suspected and could show a pulsation frequency around 26 d^{-1}. In addition, it was pointed out that the system needs high-quality data to confirm the pulsational variability. Therefore, in this study, we apply a frequency analysis to high-quality TESS data of V948 Her. Before starting the analysis, first the binary variation was removed from the light curve by fitting 32-harmonics of the orbital period frequency of 0.784 188 with the PERIOD04 code (Lenz & Breger 2005). The 32-harmonics of the orbital period frequency were chosen because they represents the binary variation well. The fit of the orbital period's harmonics was removed from the TESS data before searching for possible pulsation frequencies. A frequency

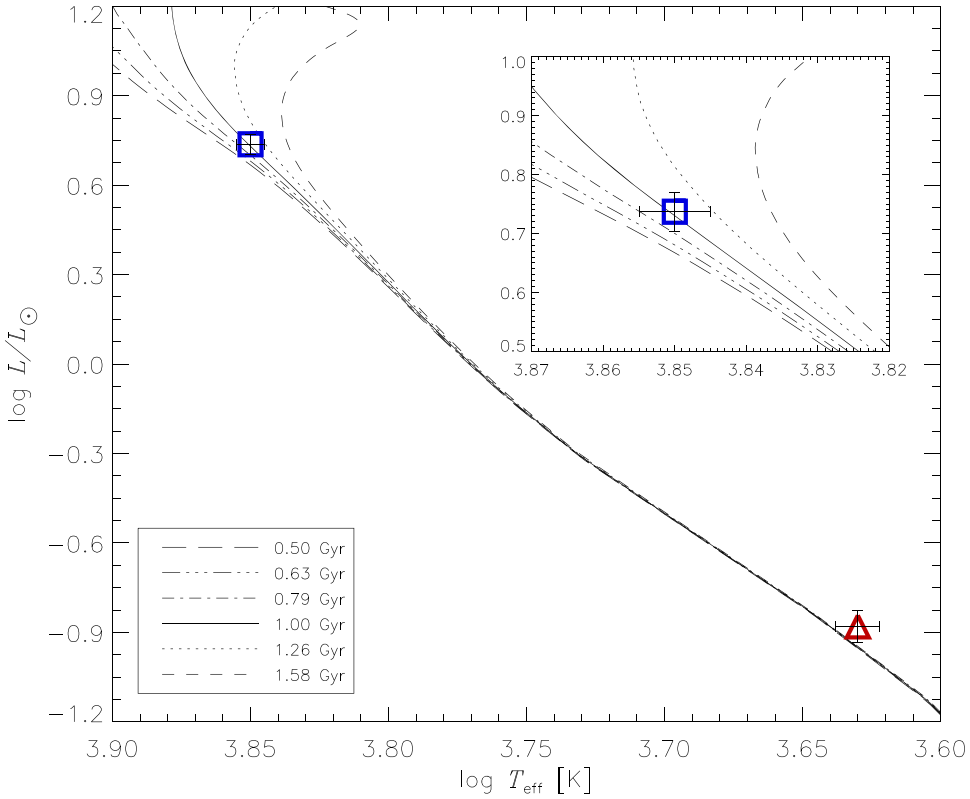

Figure 6. Isochrone for the primary (square) and secondary (triangle) components of V948 Her.

analysis was performed to the residuals with the PERIOD04 software that provides harmonics and combination frequencies. We carried out this analysis for the range of 0−80 d^{-1} until we reached the frequencies having S/N smaller than 4 (Breger et al. 1993). The resulting frequencies are listed in Table 2. As can be seen from the table, all frequencies are exactly the harmonics of the orbital period's frequency. The Fourier spectrum for this analysis is displayed in Figure 4. Except for the harmonics of the orbital period, no significant frequency with an S/N over 4 was found as depicted in the bottom panel of Figure 4. Therefore the system was defined as a non-pulsating star. With this result, we ruled out the pulsational variability of the primary component of V948 Her.

4. Discussions and Conclusion

In this study, we present the TESS light curve analysis of V948 Her. First, by using the high-quality TESS data, a binary modeling was performed with the help of results from the literature radial velocity analysis (Kahraman Aliçavus 2018). Consequently, we found a best-fitting theoretical binary modeling with a spot on the surface of the primary component. By consider the findings of the binary modeling and the results of the literature radial velocity analysis, the fundamental stellar parameters were calculated. These derived quantities are given in Table 1. When these parameters, especially the M and R values, were compared with the literature ones, significant differences were seen. In particular, the discrepancy in the M values is around 4σ. That would affect the evolution of the system.

By using the derived fundamental stellar parameters, the positions of both components in the H-R diagram were examined. The evolutionary models were taken from the MESA Isochrones and Stellar Tracks (MIST[7]) (Paxton et al. 2011; Paxton et al. 2013; Paxton et al. 2015; Dotter 2016; Choi et al. 2016). The evolutionary models were calculated for a mass range of 0.6 $M_\odot < M < 1.5$ $M_\odot$. In the model calculations, a solar abundance (Asplund et al. 2009) was assumed considering the abundance analysis result of Kahraman Aliçavus (2018). The H-R diagram for the components of V948 Her is illustrated in Figure 5. According to this diagram, the primary component's M value should be between 1.4 to 1.5 $M_\odot$, however, it was found around 1.3 $M_\odot$ in this study. This difference cannot be found for the secondary component. It it located on the evolutionary model for 0.6 $M_\odot$ which is in agreement with the secondary component's M value found in this study. To estimate the system's age, MESA isochrones were also

[7] http://waps.cfa.harvard.edu/MIST/

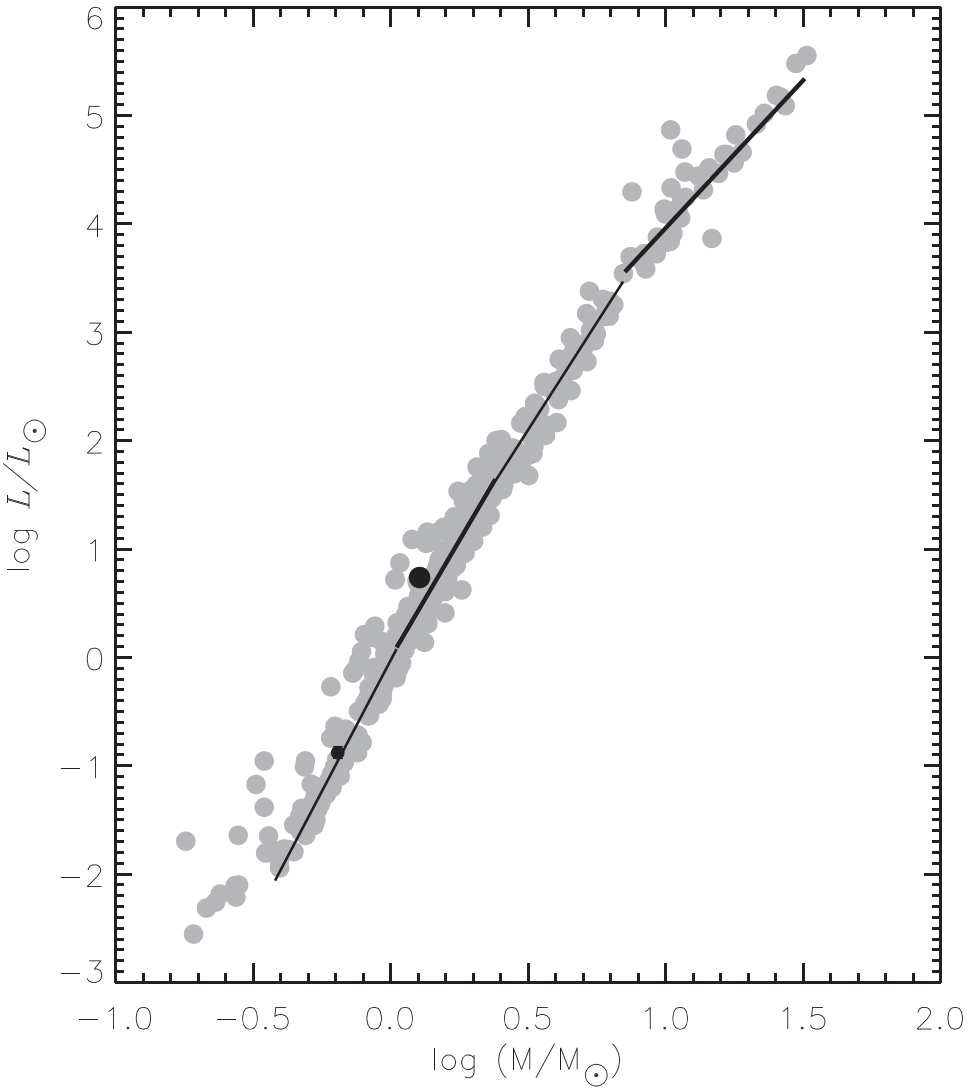

Figure 7. The position of the primary (bigger black dot) and secondary (smaller black dot) components of V948 Her in the log $M-$ log L diagram. Gray circles represent the double-lined detached eclipsing binaries given by Eker et al. (2014). The solid lines illustrate the relationships between the L and M (Eker et al. 2014).

utilized. For different ages, many isochrones with solar abundance were calculated. The positions of the primary and secondary components in the isochrone diagram are displayed in Figure 6. Taking into account the primary component's parameters, we estimated the age of the system to be 1 ± 0.24 Gyr. In Figure 7 the positions of the binary components are demonstrated in the log $M-$ log L diagram as well. This diagram was taken from Eker et al. (2014). As can be seen from the figure, both components were found to be in agreement with the general log $M-$ log L correlation.

The distance of the system was calculated using the derived fundamental parameters, the interstellar absorption value A_v (Schlafly & Finkbeiner 2011) and the bolometric correction (Eker et al. 2020). As a result, the distance of the system was found to be 164 ± 10 pc which is in agreement with the Gaia EDR3[8] distance (156 pc).

As a result of the Fourier analysis of the TESS light curve, we showed that the system does not exhibit any pulsational variation. Hence, we ruled out the pulsational characteristic of the primary component. However, when its position in the H-R diagram was examined, we found that the primary component of the system is located inside the δ Scuti instability strip (see Figure 5). This is quite interesting because it is known that a significant amount of the stars pulsate inside this instability strip, however some do not. Murphy et al. (2019) report that the pulsator fraction reaches over 70% in the middle of the δ Scuti

[8] https://gea.esac.esa.int/archive/

instability strip. This number decreases through the cool and hot borders of the instability strip and the primary component of V948 Her is placed very close to the cool border. It is now still a mystery why some stars inside the instability strip do not oscillate. To explain the existence of non-pulsators, there are some hypotheses such as wrong atmospheric parameters and chemical peculiarity. However, for V948 Her we have accurate atmospheric parameters and the chemical abundance distribution for the non-pulsating primary component. Hence, we simply rule out these hypotheses. During the research on possible pulsation frequencies, we reached the micromagnitude level and still no pulsation frequency was found. One reason for the non-pulsator in the cool border of the δ Scuti instability strip could be convection. The primary component of V948 Her is located nearly on the cool border where convection is very effective. Therefore, to accurately model the cool border of the δ Scuti instability strip, it would be better to understand the nature of pulsating and non-pulsating stars placed close to this area. For this reason, more samples of non-pulsating stars, with precise fundamental parameters, are requested. Therefore, eclipsing binary systems are unique because they allow us to determine sensitive fundamental parameters and examine their evolutionary status. V948 Her is one of these systems that allow us to understand the reason why some systems inside the δ Scuti instability strip do not pulsate.

Acknowledgments

We would like to thank the reviewer for useful comments and suggestions that helped to improve the publication. This study has been supported by the Scientific and Technological Research Council (TUBITAK) project through 120F330. The authors thank Dr. Gerald Handler for discussions and his valuable suggestions. The TESS data presented in this paper were obtained from the Mikulski Archive for Space Telescopes (MAST). Funding for the TESS mission is provided by the NASA Explorer Program. This paper makes use of data from the first public release of the WASP data (Butters et al. 2010) as provided by the WASP consortium and services at the NASA Exoplanet Archive, which is operated by the California Institute of Technology, under contract with the National Aeronautics and Space Administration under the Exoplanet Exploration Program. This research has made use of the SIMBAD database, operated at CDS, Strasbourg, France. This work has made use of data from the European Space Agency (ESA) mission Gaia (https://www.cosmos.esa.int/gaia), processed by the Gaia Data Processing and Analysis Consortium (DPAC, https://www.cosmos.esa.int/web/gaia/dpac/consortium). Funding for the DPAC has been provided by national institutions, in particular the institutions participating in the Gaia Multilateral Agreement.

Table A.1
The Minima Times Derived from the TESS and SuperWASP Data and Taken from O-C Gateway. I and II Represent the Primary and Secondary Minimums Respectively

Time of minima HJD (2400000+)	Minima type	Reference
48501.1070	I	ESA (1997)
51318.0650	I	1
53173.4690 ± 0.0004	I	Aksu et al. (2005)
54943.4551 ± 0.0005	I	Brat et al. (2009)
55360.4494 ± 0.0005	I	Liakos & Niarchos (2010a)
55365.5491 ± 0.0002	I	Liakos & Niarchos (2010a, 2010a)
55376.3885 ± 0.0013	II	Liakos & Niarchos (2010b)
56815.4574 ± 0.0005	I	Honkova et al. (2015)
57139.3638 ± 0.0014	I	Juryšek et al. (2017)
54642.50739 ± 0.00009	I	SuperWASP
54647.60967 ± 0.00030	I	SuperWASP
54656.53481 ± 0.00020	I	SuperWASP
54665.46272 ± 0.00020	I	SuperWASP
58984.58299 ± 0.00003	I	TESS
58997.33502 ± 0.00002	I	TESS
59008.81193 ± 0.00002	I	TESS
59011.36230 ± 0.00002	I	TESS
59021.56400 ± 0.00002	I	TESS
59034.31609 ± 0.00002	I	TESS
58983.94627 ± 0.00022	II	TESS
58994.14778 ± 0.00011	II	TESS
59008.17487 ± 0.00020	II	TESS
59010.72816 ± 0.00090	II	TESS
59023.47770 ± 0.00013	II	TESS
59033.67918 ± 0.00012	II	TESS
59405.40676 ± 0.00020	I	This study

ORCID iDs

F Kahraman Aliçavuş, https://orcid.org/0000-0002-9036-7476

References

Aksu, O., Ozavci, I., Yuce, K., et al. 2005, IBVS, 5588, 1
Antoci, V., Cunha, M., Houdek, G., et al. 2014, ApJ, 796, 118
Asplund, M., Grevesse, N., Sauval, A. J., & Scott, P. 2009, ARA&A, 47, 481
Baglin, A., Auvergne, M., Boisnard, L., et al. 2006, in XXXVI COSPAR Scientific Assembly, 36, 3749
Balona, L. A., & Dziembowski, W. A. 2011, MNRAS, 417, 591
Borucki, W. J., Koch, D., Basri, G., et al. 2010, Sci, 327, 977
Bowman, D. M., & Kurtz, D. W. 2018, MNRAS, 476, 3169
Brat, L., Trnka, J., Lehky, M., et al. 2009, OEJV, 107, 1
Breger, M. 1969, ApJS, 19, 79
Breger, M., Stich, J., Garrido, R., et al. 1993, A&A, 271, 482
Butters, O. W., West, R. G., Anderson, D. R., et al. 2010, A&A, 520, L10
Choi, J., Dotter, A., Conroy, C., et al. 2016, ApJ, 823, 102
Dotter, A. 2016, ApJS, 222, 8
Dupret, M.-A., Grigahcène, A., Garrido, R., Gabriel, M., & Scuflaire, R. 2005, A&A, 435, 927
Eigmüller, P., Csizmadia, S., Endl, M., et al. 2018, MNRAS, 480, 3864
Eker, Z., Bilir, S., Soydugan, F., et al. 2014, PASA, 31, e024
Eker, Z., Soydugan, F., Bilir, S., et al. 2020, MNRAS, 496, 3887

ESA 1997, ESA Special Publication, 1200
Guzik, J. A., Bradley, P. A., Jackiewiecz, J., et al. 2013, AstRv, 8, 83
Herrero, E., Lanza, A. F., Ribas, I., et al. 2014, A&A, 563, A104
Honkova, K., Jurysek, J., Lehky, M., et al. 2015, OEJV, 168, 1
Juryšek, J., Hoňková, K., Šmelcer, L., et al. 2017, OEJV, 179, 1
Kahraman Aliçavus, F. 2018, RAA, 18, 087
Kwee, K. K., & van Woerden, H. 1956, BAN, 12, 327
Lenz, P., & Breger, M. 2005, CoAst, 146, 53
Liakos, A., & Niarchos, P. 2010a, IBVS, 5943, 1
Liakos, A., & Niarchos, P. 2010b, IBVS, 5958, 1
Liakos, A., & Niarchos, P. 2012, NewA, 17, 634
Maxted, P. F. L., Gaulme, P., Graczyk, D., et al. 2020, MNRAS, 498, 332
Murphy, S. J., Bedding, T. R., Niemczura, E., et al. 2015, MNRAS, 447, 3948
Murphy, S. J., Hey, D., Van Reeth, T., et al. 2019, MNRAS, 485, 2380
Narloch, W., Pietrzyński, G., Kołaczkowski, Z., et al. 2019, MNRAS, 489, 3285
Pan, Y., Fu, J.-N., Zong, W., et al. 2020, ApJ, 905, 67
Paxton, B., Bildsten, L., Dotter, A., et al. 2011, ApJS, 192, 3
Paxton, B., Cantiello, M., Arras, P., et al. 2013, ApJS, 208, 4
Paxton, B., Marchant, P., Schwab, J., et al. 2015, ApJS, 220, 15
Ricker, G. R., Winn, J. N., Vanderspek, R., et al. 2014, Proc. SPIE, 9143, 914320
Schlafly, E. F., & Finkbeiner, D. P. 2011, ApJ, 737, 103
Soydugan, E., Soydugan, F., Demircan, O., & İbanoğlu, C. 2006, MNRAS, 370, 2013
Tkachenko, A., Pavlovski, K., Johnston, C., et al. 2020, A&A, 637, A60
Torres, G., Andersen, J., & Giménez, A. 2010, A&Ar, 18, 67
Uytterhoeven, K., Moya, A., Grigahcène, A., et al. 2011, A&A, 534, A125
Wilson, R. E., & Devinney, E. J. 1971, ApJ, 166, 605
Zasche, P., Liakos, A., Niarchos, P., et al. 2009, NewA, 14, 121
Zola, S., Rucinski, S. M., Baran, A., et al. 2004, AcA, 54, 299
Zola, S., Gazeas, K., Kreiner, J. M., et al. 2010, MNRAS, 408, 464